# Role of CD200/CD200R Signaling Pathway in Regulation of CD4+T Cell Subsets During Thermal Ablation of Hepatocellular Carcinoma

Authors' Contribution:
Study Design A
Data Collection B
Statistical Analysis C
Data Interpretation D
Manuscript Preparation E
Literature Search F
Funds Collection G

ABCDE 1 **Shengchuan Huang**
ABC 1 **Yan Pan**
ABCE 1 **Qingdong Zhang**
ABD 2 **Weiping Sun**

1 Department of Ultrasonics, The Affiliated Yantai Yuhuangding Hospital of Qingdao University, Yantai, Shandong, P.R. China
2 Department of Geriatric Medicine, Haiyang People's Hospital, Yantai, Shandong, P.R. China

Corresponding Author: Weiping Sun, e-mail: wpl852@126.com
Source of support: Departmental sources

**Background:** In this study, we assessed the role of CD200 and CD200 receptor (CD200R) in regulating CD4+T cell subsets and assessed the therapeutic efficacy of thermal ablation for liver hepatocellular carcinoma (HCC) in rats.

**Material/Methods:** Seventy-eight male C57BL/6 rats were randomly divided into 7 groups: a control group, a model group, a CD200FC group, an anti-CD200R1 mAb group, a thermal ablation group, a thermal ablation+CD200 FC group, and a thermal ablation+anti-CD200R1 mAb group. The levels of CD200, CD200R1, Th1, Th17, and Treg in peripheral blood were detected by flow cytometry. Immunohistochemistry was used to detect CD200, CD200R1, IFN-γ, IL-17, Foxp3 protein expression in tumor tissues.

**Results:** The levels of CD200, CD200R1, Th17, and Treg were significantly increased after CD200FC treatment (p<0.05). After treatment with anti-CD200R1 mAb, the levels of CD200, CD200R1, Th17, and Treg decreased and Th1 increased. Compared with the control group, the expression of CD200, CD200R1, IL-17, and Foxp3 in the model group increased significantly, and the expression of IFN-γ decreased significantly (p<0.05). The expression of CD200, CD200R1, IL-17, and Foxp3 was significantly reduced by adding anti-CD200R1 mAb, and the expression of IFN-γ was increased (p<0.05). After the thermal ablation treatment, the proteins continued to decrease and the expression of IFN-γ continued to increase.

**Conclusions:** The CD200/CD200R pathway participates in HCC tumor growth and the expression of CD4+T cell subsets in cancer tissues. Furthermore, thermal ablation treatment inhibited cancer recurrence.

**MeSH Keywords:** **Acquired Immunodeficiency Syndrome • Liver Diseases, Alcoholic • T-Lymphocytes, Regulatory**

**Full-text PDF:** https://www.medscimonit.com/abstract/index/idArt/913094

📄 3019    📊 — 📈 7    📑 31

## Background

Liver hepatocellular carcinoma (HCC) is an important and common malignancy in China, involving the carcinogenesis of hepatocytes and intrahepatic bile duct epithelial cells [1]. The prognosis of patients with HCC is poor because of the high recurrence rate, and HCC accounts for about 80–90% of hepatocellular carcinoma cases [2].

The rapid development of thermal ablation is an important breakthrough in the nonsurgical resection of tumors, and it has become the third most used potentially curative method to treat HCC. Some patients have liver cancer that cannot be excised and some HCC cannot be resected, such as severe chlorosis and tumor invasion of major vascular pedicles [3,4], and even after resection, the recurrence rate is high and the local recurrence rate at 9 months is up to 11% [5], which is a problem with thermal ablation treatment. Ali et al. demonstrated that thermal ablation can induce the exposure of tumor cell antigens to some extent, thus inducing active immunity [6].

CD200 and CD200 receptor (CD200R) play an important role in the immune system [7]. The signal pathway is mainly mediated by myeloid cells to indirectly regulate immune balance. It may play an important role in allergy, immune system function, central nervous system injury, transplantation rejection, and other immune-related diseases [8,9]. The expression of CD200 and CD200R in patients with HCC is significantly higher than in the general population [10]. The CD200R pathway can lead to immune tolerance that inhibits the immune function in patients with HCC [11]. Therefore, we studied the role of the CD200/CD200R pathway on CD4+T cell subsets of HCC and assessed the effect of thermal ablation on HCC in rats.

## Material and Methods

### Cell culture

Hepa1-6 (CRL-1830, ATCC, USA) cells stored in liquid nitrogen were removed and the cryopreservation tube was immediately thawed in a preheated water bath. After 1–2 min, the liquid in the cryopreservation tube was completely dissolved, then removed, and we wiped the outer wall of the cryopreservation tube with a cotton ball. After 1000 rpm centrifuge for 3 min, we discarded the supernatant, added 10 mL medium into the centrifuge tube to make a cell suspension. The cell concentration was adjusted to $5\times10^5$/mL, and the cell suspension was separated in the culture bottle at 37°C in a 5% $CO_2$ incubator (Thermo Fisher Scientific, USA). After 24–48 h, the liquid was changed and culturing was continued. When the cells in the bottle grew to 80–90%, the culture liquid was tilted and rinsed. At 37°C, 2.5 g/L trypsin (Invitrogen, Carlsbad, CA, USA) was used

to digest the cells, which became crinkled and rounded, and the trypsin was tilting. We added 1 mL serum-free medium to form a cell suspension, followed by centrifugation at 800 rpm for 3 min. We discarded the supernatant, then added the serum-free medium to resuspend the cells and mix them. Trypan blue staining was used to count the cells, and the ratio of viable cells was more than 95%. We mixed of $2\times10^{10}$/L of cell suspension with PBS solution.

### Animals

Seventy-eight male C57BL/6 mice (purchased from Ji'nanPengYue Experimental Animal Breeding Co., license number SCXK (Lu) 2014-0007), weight (18±2) g, 4–6 weeks of age, were kept at 22–24°C and relative humidity of 50–60% in a well-ventilated and quiet environment in an SPF-class animal room, with free access to water and feed. Animal experiments followed the NIH guidelines (NIH Pub. No. 85-23, revised 1996) and were approved by the Qingdao University Animal Protection and Use Committee.

### Establishment of mouse liver cancer model and animal grouping

The right axillary skin of the mice was sterilized by 95% alcohol, and 0.1 mL of cell suspension was injected under aseptic conditions. During the injection, the skin was slowly swollen and gradually formed into a circular mound, then we pulled out the needle. C57BL/6 mice were fed under suitable conditions, and the mice were anesthetized by intraperitoneal injection with pentobarbital sodium (70 mg/kg) on day 1 and day 7. Then, mice were fixed on a special operating table. The tumors were fixed with the tweezers, then small needle heads were inserted along the long axis of the tumor and the tip of the needle was located at the center of the tumor. The following operations are followed: (1) In the control group, C57BL/6 mice were normally reared under suitable conditions; (2) In the model group (Model), mice received rapid injection of 0.15 mL normal saline at the tumor site; (3) In the CD200FC group, 20 ng/ml CD200FC was injected at the tumor site; (4) In the anti-CD200R1 mAb group, 20 ng/ml anti-CD200R1 mAb was injected at the tumor site; (5) In the thermal ablation (T) group, mice received rapid injection of 0.15 mL normal saline heated to 50°C at the tumor site; (6) In the T+CD200 FC group, mice received multiple injections of 0.15 mL normal saline heated to 50°C at the tumor site, and 20 ng/ml CD200FC 10 min after injection at the tumor site; (7) In the T+anti-CD200R1 mAb group, mice received multiple injections of 0.15mL normal saline heated to 50 °C at the tumor site, and 20 ng/mL anti-CD200R1 mAb 10 min after injection at the tumor site.

### Inhibition rate

After treatment, the mice in each group were assessed for volume of liver cancer with vernier calipers every 3 day, the tumor growth curve within 15 days was drawn, and the tumor inhibition rate was calculated. Tumor volume was calculated as $V=a \times b^2/2$ (a: tumor long diameter; b: tumor short diameter). Tumor volume inhibition rate was calculated as (%)=(average volume of Model group–average volume of experimental group)/average volume of Model group×100%

### Inoculation

The surviving mice were divided into 6 mice per group, and then 0.1 mL of Hepa1-6 hepatoma cell suspension with a concentration of $2 \times 10^{10}$/L was injected into the left axillary. After 7 days, the tumor growth volume was observed and the recurrence of liver cancer was observed. The levels of CD200, CD200R1, Th1, Th17, and Treg in the peripheral blood were detected.

### The numbers of CD200, CD200R1, Th1, Th17, and Treg cells in peripheral blood were detected by flow cytometry.

We collected blood from the orbits of the mice before treatment, 7 days after treatment, and 15 days after treatment. For assessment of CD200 and CD200R1, we used anticoagulant in whole blood for a total volume of 200 μl per tube. After lysis by Red Blood Cell Lysis Buffer (Beijing Solarbio Science and Technology Co., Beijing, China), cells were resuspended in PBS. We added 10 μL CD38-FITC (FITC anti-mouse CD38, Bioscience, USA) and 10 μL CD15-FITC (FITC anti-mouse). After mixing, tubes were incubated in the dark at room temperature for 30 min. After washing 2 times, fixing, and permeabilization, we added 10 μL CD200-PE (PE anti-mouseCD200, eBioscience, USA) and CD200R1-PE (PE anti-mouseCD200R1, eBioscience, USA), followed by mixing, and incubating for 30 min at room temperature. After washing, FACS Canto II flow cytometry (BD, USA) was performed.

For Treg cell staining, we used anticoagulant in whole blood for 200 μL per tube, and after lysis by Red Blood Cell Lysis Buffer (Beijing Solarbio Science and Technology Co., Beijing, China), cells were resuspended in PBS. Then, we added 10 μL each CD4-FITC (FITC anti-mouse CD4, eBioscience, USA) and CD25-APC (APC anti-mouseCD25, eBioscience), followed by mixing and incubation at room temperature in the dark for 30 min. After washing 2 times, cells were fixed and permeabilized, the we added 10 μL Foxp3-PE (PE anti-mouse Foxp3, eBioscience, USA), followed by incubation for 30 min at room temperature.

For Th1 and Th17 cell staining, anticoagulant whole blood for 200 μL per tube, after lysis by Red Blood Cell Lysis Buffer (Beijing Solarbio Science & Technology Co. Beijing, China) were

resuspended in PBS. Then added 10 μL CD4-FITC, concussion was mixed and incubated at room temperature for 30 min. Two times of washing, fixed and permeable, adding 10 μL IFN-γ-PE (PE anti-mouse IFN-γ, eBioscience, USA) and 10 μL IL-l7-PE (PE anti-mouse IL-17, eBioscience, and IL-l7-PE), concussion and mixed, and incubated 30 at room temperature. After washed, tested on the machine.

### Immunohistochemistry was used to detect the expression of CD200, CD200R1, IFN-γ, IL-17, Foxp3 proteins in tumor tissues

After 15 days of thermal ablation, the mice were killed by the neck breaking method after anesthetized by intraperitoneally injected with pentobarbital sodium (70 mg/kg). After routine sections of the tumor tissue, the roasted tablets were dewaxed with xylene, followed by gradient ethanol solution hydration. The high temperature antigen in citric acid buffer was used to repair 20 min and 5% BSA was used to block 20 min. Rabbit anti-Mouse CD200 (ABIN2878047, antibodies-online), rabbit anti-mouse CD200R1 polyclonal antibody (orb352595, Biorbyt, USA), rabbit Anti-Interferon gamma polyclonal antibody (ab9657, Abcam, USA), rabbit anti-mouse IL-17 polyclonal antibody polyclonal antibodies (ABIN1862735, Biorbyt, USA) and rabbit anti-mouse Foxp3 polyclonal antibodies (ABIN2506653, Biorbyt, USA) were reacted at 4°C for the night, and PBS flushed 3 min for 3 times. After rewarming, hatching of Goat anti-rabbit IgG (Proteintech, USA) labeled with horseradish peroxidase was performed. DAB was coloured, and hematoxylin was slightly restained, dehydrated, transparent, and neutral gum seal. Each of the 3 slices was observed under an optical microscope (Olympus, Japan, ×400).

### Statistical analyses

The SPSS19.0 statistics software was used to analyze the monitoring data, and the data analysis results were all expressed as mean ± standard deviation (mean ±SD). The data analysis between the 2 groups was tested by *t* test. Multiple comparisons were analyzed by single factor analysis of variance (ANOVA), followed by SNK test, and the difference was statistically significant by *p<0.05*.

## Results

### Growth of subcutaneous tumor in mice

After subcutaneous inoculation of Hepa1-6 cells, the model mice were stable, the tumor formation rate was 100%, and the tumor growth was rapid. From the 2nd inoculation, all the subcutaneous nodules were visible to the naked eye. The average diameter of the tumor could reach 6-8 mm on the 8th day.
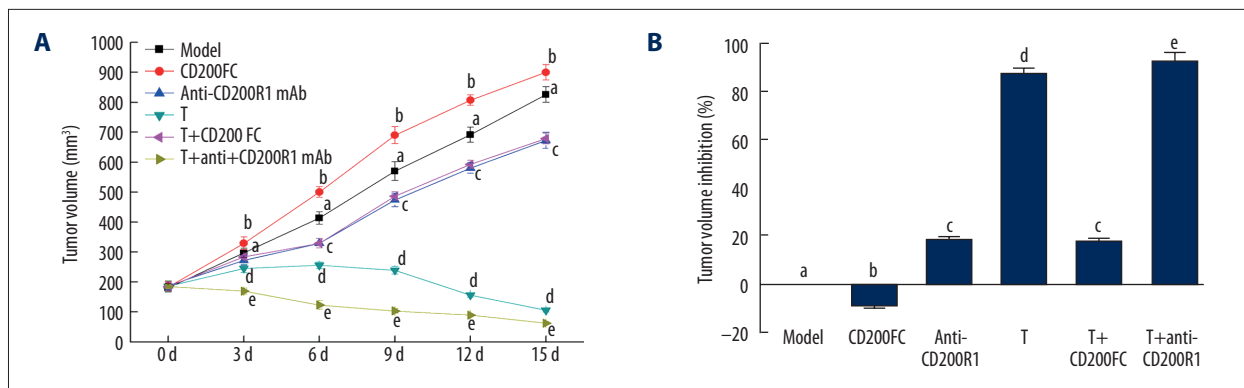
**Figure 1.** Growth of subcutaneous tumors in mice. (**A**) Volume change; (**B**) Tumor volume inhibition rate. The data are displayed as the mean ±SD (n=6). Different letters represent significant differences between groups (p<0.05).

Then start the experiment, the tumor tissues were obtained after thermal ablation for 15 days. The single factor analysis of variance showed that the size of the transplanted tumor in all the experimental groups was significantly different from that of the Model group ($p<0.05$), and the difference was significant (except for anti-CD200R1 mAb and T+CD200FC 2 groups) ($p<0.05$) (Figure 1A, 1B). Compared with model group (180.37±14.44, 825.66±26.40), adding CD200FC significantly promoted tumor growth (183.63±14.23, 899.86±25.32), the difference was statistically significant ($p<0.05$), and anti-CD200R1 mAb significantly inhibited tumor growth, the tumor volume only grew to 473.86±22.96 mm³, and its inhibitory rate was 18.55%, the difference was statistically significant ($p<0.05$). After thermal ablation thermal ablation, the growth of mice transplanted tumor was obviously inhibited, and the effect of the treatment was obvious (185.63±18.08, 105.61±6.54), the inhibitory rate was 87.21%, the difference was statistically significant ($p<0.05$). After the thermal ablation thermal ablation, the tumor growth was suppressed by adding CD200FC, the tumor was inhibited, but there was no obvious therapeutic effect. The inhibition rate dropped to 17.76%, and there was no significant difference between the anti-CD200R1 mAb group and the group ($p>0.05$). After the thermal ablation thermal ablation, anti-CD200R1 mAb was added to the treatment (185.21±16.12, 62.17±2.50), the tumor volume inhibition rate was 92.47%, and the therapeutic effect was significant ($P<0.05$) (Figure 2). The results indicate that CD200/CD200R signaling pathway plays a regulatory role in the thermal ablation of hepatocellular carcinoma.

**Numbers of CD200, CD200R1, Th1, Th17 and Treg cells in peripheral blood**

As shown in Figure 3–5, the cell frequency in each group before treatment was significantly different from that of the control group, of which the contents of CD200, CD200R1, Th17 and Treg increased significantly, and the content of Th1 decreased significantly ($p<0.05$) (Figure 3). After the treatment of 7d, the cell frequency of CD200, CD200R1 and CD200R1 were significantly increased after the CD200FC treatment. After anti-CD200R1 mAb treatment, the contents of CD200, CD200R1, Th17 and Treg decreased, while the content of Th1 increased ($p<0.05$). After the thermal ablation treatment, the contents of CD200, CD200R1 and Th17 were obviously reduced, and the content of Th1 was increased. There was no significant difference in the anti-CD200R1 mAb group ($p>0.05$) (Figure 4). After the thermal ablation combined with anti-CD200R1 mAb, the contents of CD200, CD200R1, Th17 and Treg were reduced, and the content of Th1 was increased ($p<0.05$), and there was no significant difference in the content after the treatment of 15 days (Figure 5).

**Immunohistochemistry was used to detect the expression of CD200, CD200R1, Th1, Th17 and Treg proteins in tumor tissues.**

The expression level of related proteins in tumor tissue was detected by immunohistochemistry. As shown in Figure 5, CD200 and CD200R1 were mainly expressed in the matrix area around the liver cancer tissue, and the cytokine IFN-γ of Th1 was mainly expressed in the cytoplasm. The cytokine IL-17 of Th17 was positive in cytoplasm and nucleus of the cell, and Treg specific transcription factor Foxp3 was expressed in nucleus (Figure 5A). The expression of CD200 and CD200R1 in the control group was weakly positive or almost non-existent. Compared with the control group, the expression of CD200, CD200R1 IL-17, and Foxp3 in the tumor tissues of the model group increased significantly, and the expression of IFN-γ protein decreased significantly ($p<0.05$). After CD200FC treatment, the expression of CD200, CD200R1, IL-17, and Foxp3 protein were strongly positive, which was significantly higher than that of the model group ($p<0.05$), while the expression of IFN-γ protein was obviously inhibited compared with the model group ($p<0.05$). The expression of CD200, CD200R1, IL-17, and Foxp3 proteins was significantly downregulated by anti-CD200R1 mAb, and the difference was statistically significant.
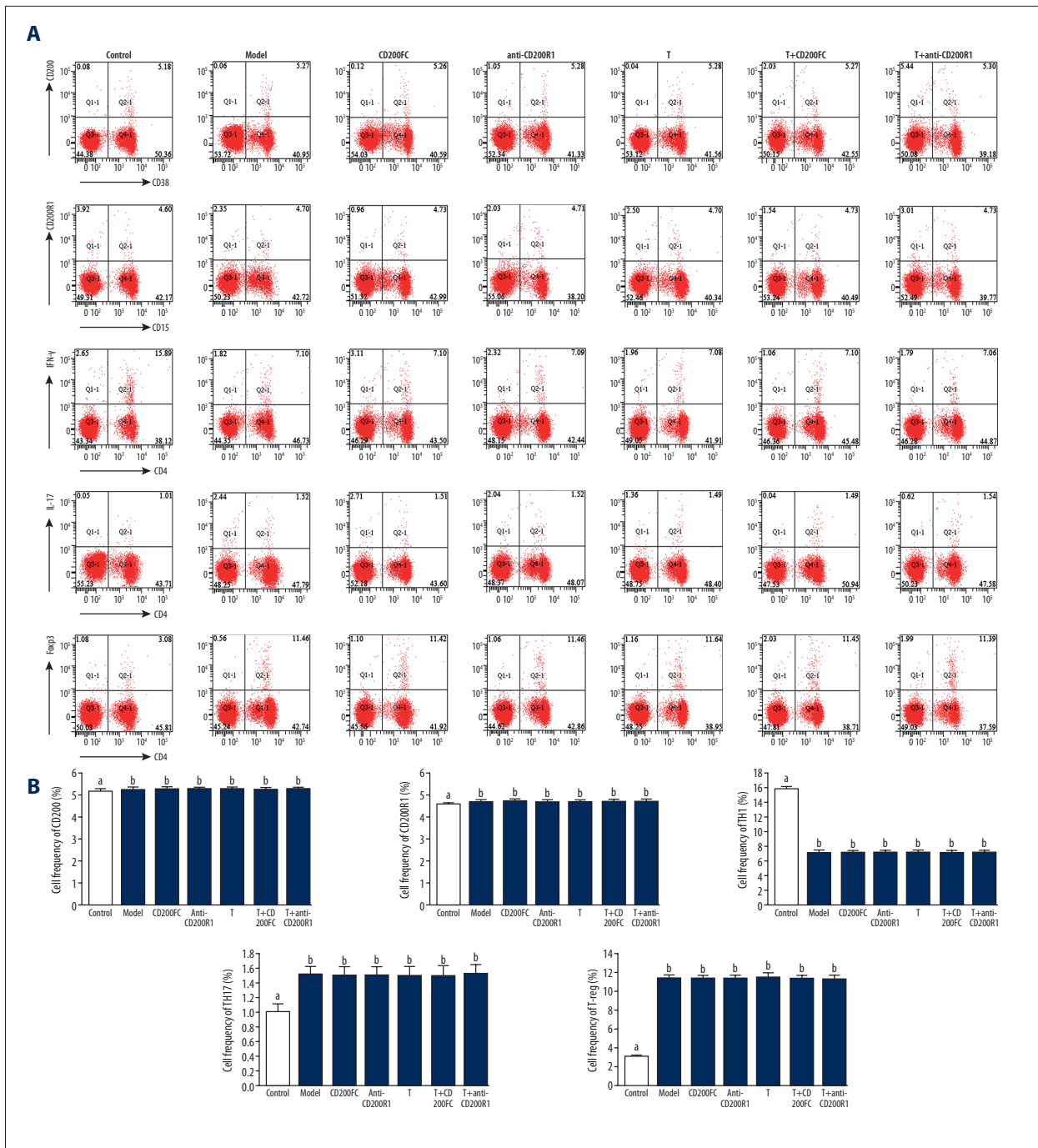
**Figure 2.** Frequencies of CD200, CD200R1, Th1, Th17, and Treg cells in peripheral blood before treatment. (**A**) Flow cytometry; (**B**) Cell frequency. The data are displayed as the mean ±SD (n=6). Different letters represent significant differences between the groups (p<0.05).

After thermal ablation, the positive expression of 4 proteins – CD200, CD200R1, IL-17, and Foxp3 – continued to decrease, and the positive expression of IFN-γ continued to increase, and the difference was statistically significant (*p<0.05*). After the thermal ablation, the expression level of the 5 proteins was not significantly different from the anti-CD200R1 mAb group,

and the heat dissipated (*p>0.05*). After thawing and combining with anti-CD200R1 mAb, the expression of 4 proteins – CD200, CD200R1, IL-17, and Foxp3 – was weakly positive, while IFN-γ proteins were strongly positive, and there was no significant difference compared with the control group (*p>0.05*), indicating that the therapeutic effect was significant (Figure 5B).
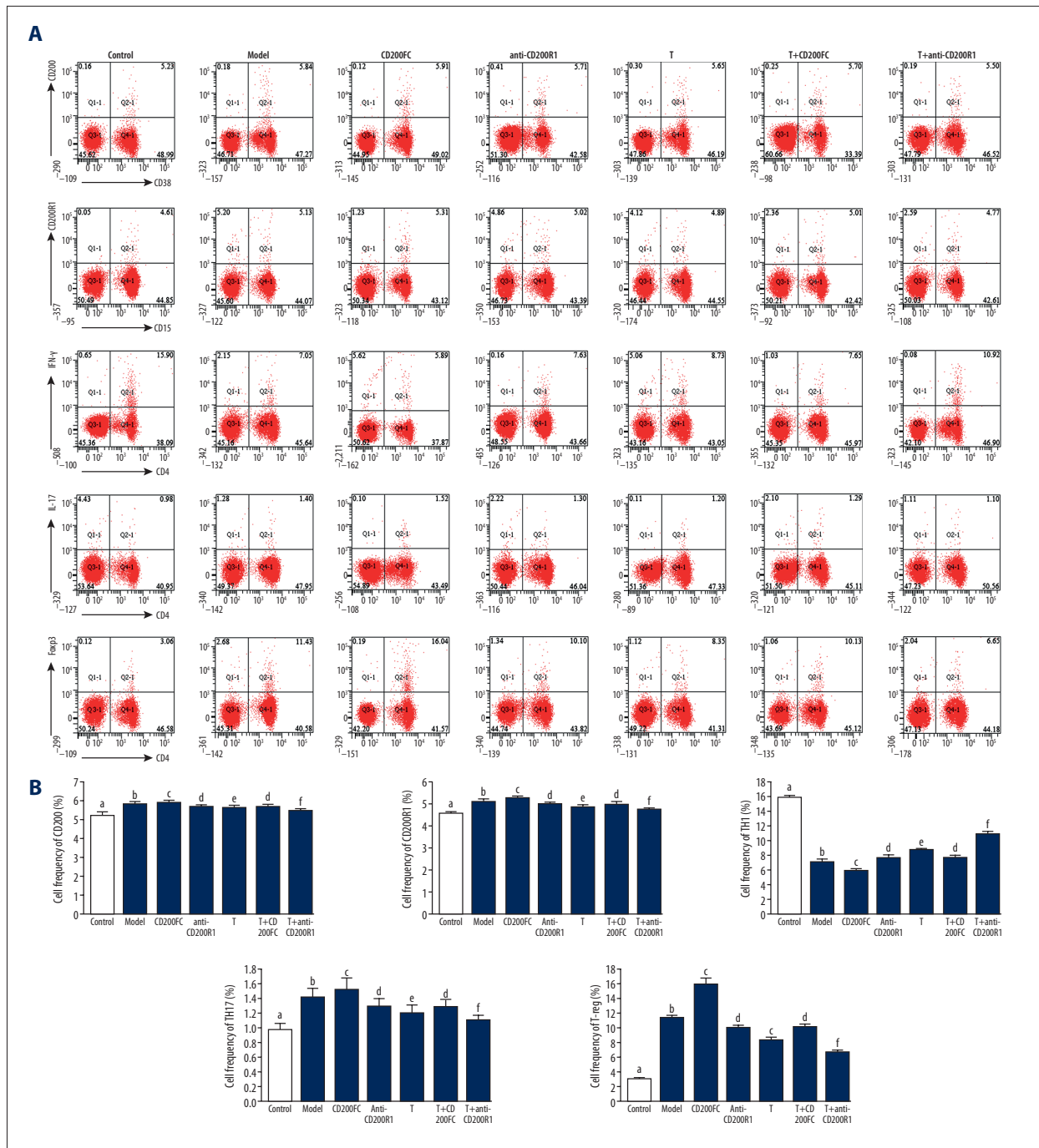
**Figure 3.** Frequency of CD200, CD200R1, Th1, Th17, and Treg cells in peripheral blood after 7 days of treatment. (**A**) Flow cytometry; (**B**) Cell frequency. The data are displayed as the mean ±SD (n=6). Different letters represent significant differences between the groups (p<0.05).

### Detection of recurrence rate of liver cancer

The right axillary contralateral inoculation method was used to detect the recurrence of HCC in mice. The results are shown in Figure 6. The tumor size of all experimental groups was significantly different from that of the model group after re-inoculation (*p<0.05*). Compared with the model group (173.8±7.29), the recurrence rate of liver cancer in the CD200FC group was 100% and the tumor growth was obvious. The size of the tumors was 294.22±18.52 mm³ after 7 days, and the recurrence rate in the anti-CD200R1 mAb group was 100% but the tumor growth was significantly slowed, and the size
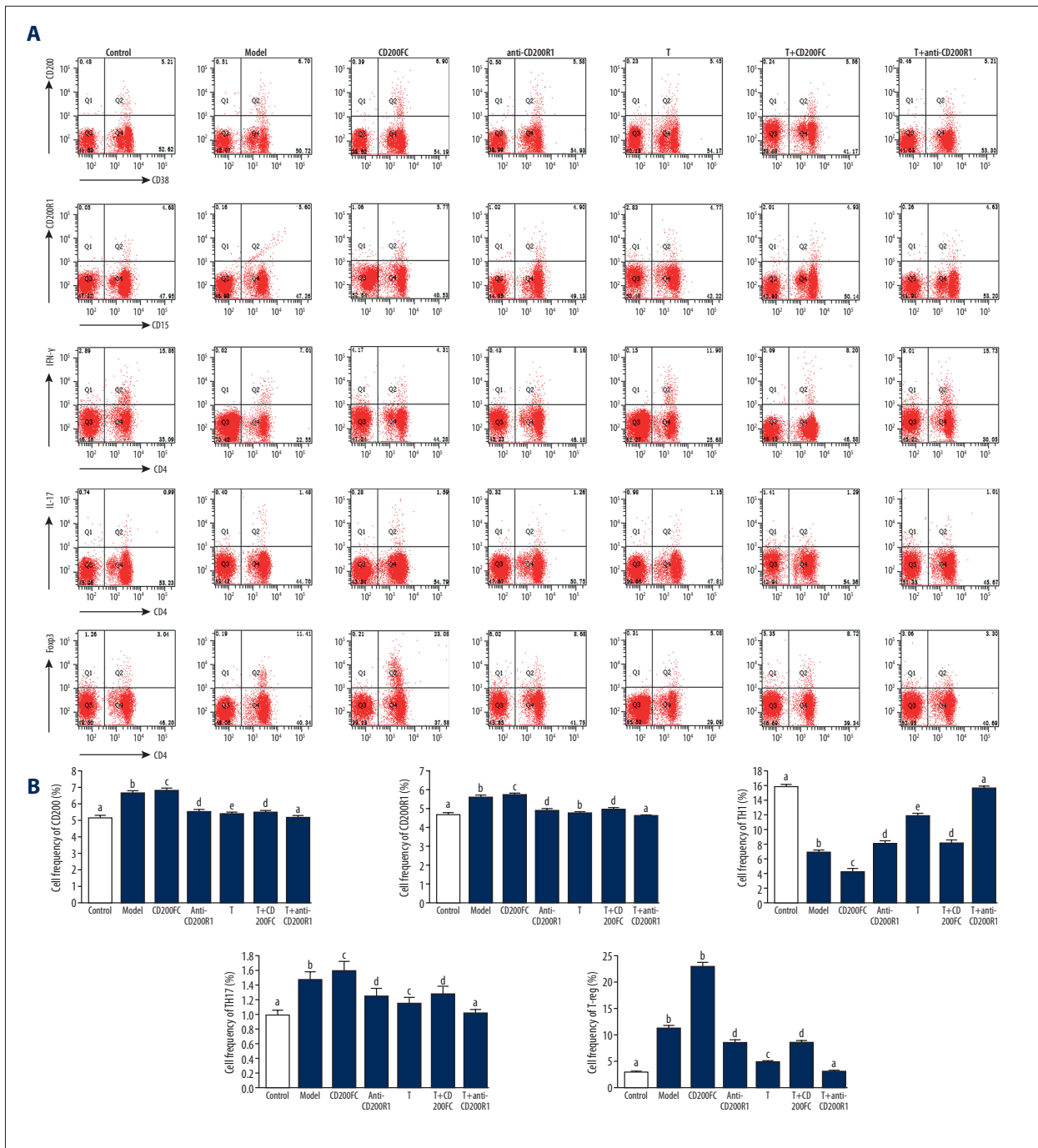
**Figure 4.** Frequencies of CD200, CD200R1, Th1, Th17, and Treg cells in peripheral blood after 15 days of treatment. (**A**) Flow cytometry; (**B**) Cell frequency. The data are displayed as the mean ±SD (n=6). Different letters represent significant differences between groups (p<0.05).

of the tumors was 51.55±2.67 mm³ after 7 days. After inoculation, the effect of early treatment was better, and only 1 mouse had no recurrence of liver cancer. The average volume of tumors was 4.93 ± 2.23mm³ after 7 days, and there was no significant difference between the recurrence of HCC and the size of anti-CD200R1 mAb in the T+CD200FC group (*p>0.05*).

After the re-inoculation of T+anti-CD200R1 mAb mice, 4 mice had no recurrence, and the average size of tumors after 7 days was only 0.33±0.47 mm³.
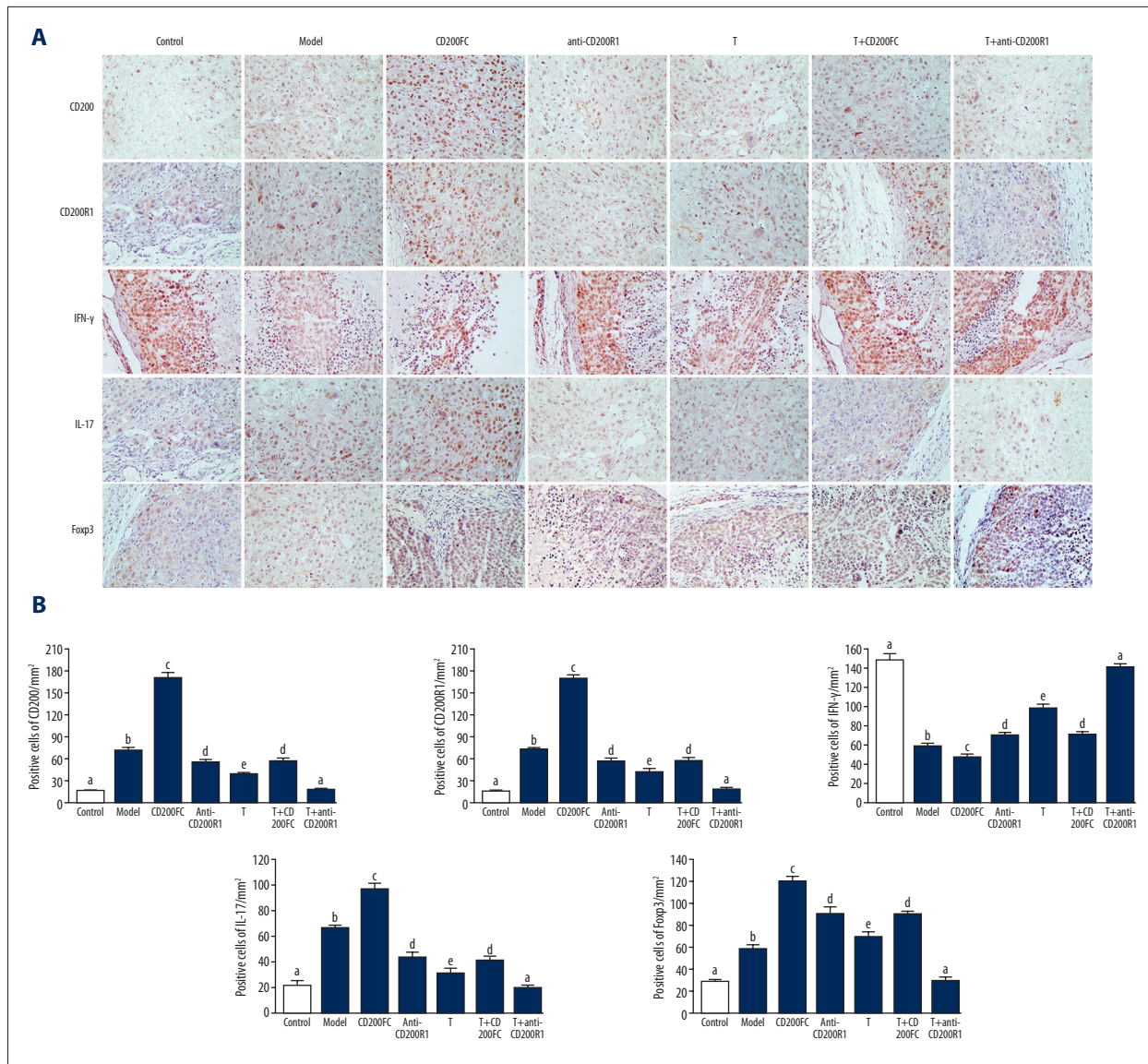
**Figure 5.** The expression levels of CD200, CD200R1, IFN-γ, IL-17, and Foxp3 proteins in tumor tissues were detected by immunohistochemistry. (**A**) Immunohistochemical staining; (**B**) The number of protein-positive cells in tumor tissue. Data are displayed as mean ±SD (n=3). Note: different letters represent significant differences between groups (p<0.05).
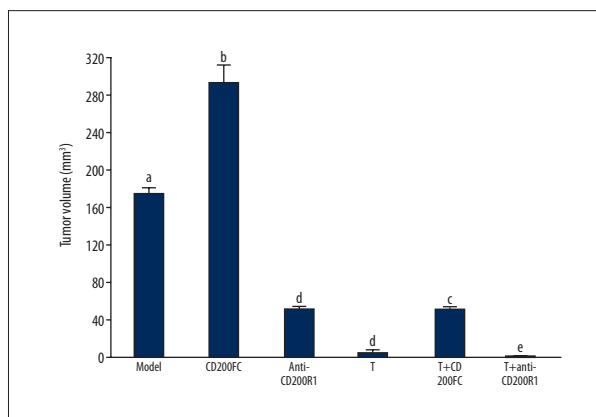


**Figure 6.** Tumor growth after subcutaneous re-inoculation in mice. The data are displayed as mean ±SD (n=6). Note: different letters represent significant differences between the groups (p<0.05).

## Cell numbers of CD200, CD200R1, Th1, Th17, and Treg cells in peripheral blood

Figure 7 shows the cell numbers of each group at 7 days after re-inoculation. There was no significant difference in the cell numbers between the T+anti-CD200R1 mAb group and the control group, indicating that the early treatment effect was significant.

**Figure 7.** The frequency of related cells in peripheral blood 7 days after re-inoculation. (**A**) Flow cytometry; (**B**) Cell frequency. The data are displayed as mean ±SD (n=6). Different letters represent significant differences between the groups (p<0.05).

## Discussion

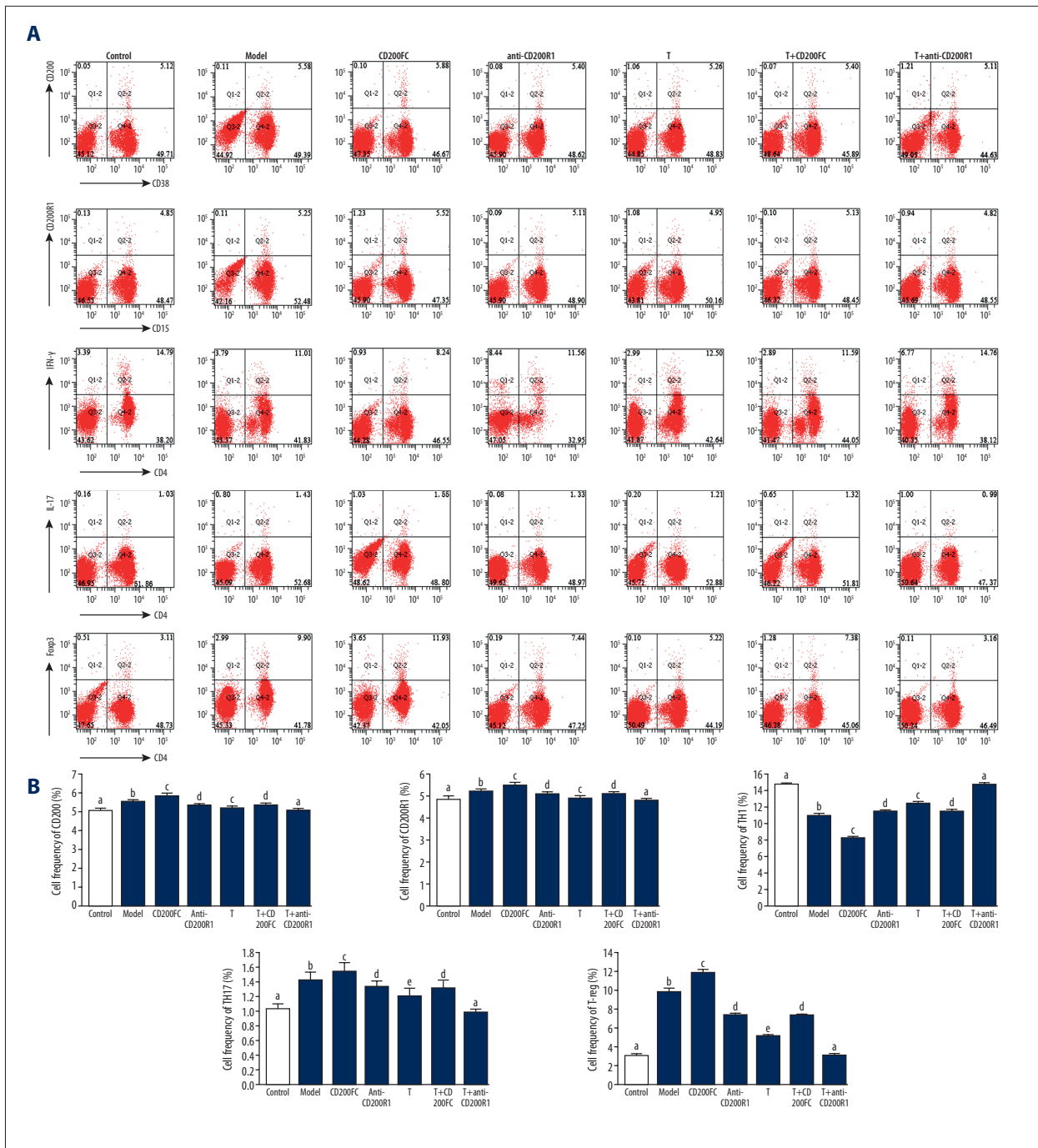Hepatocellular carcinoma (HCC) accounts for about 80–90% of all cases of hepatocellular carcinoma, followed by cholangiocarcinoma and mixed hepatocellular cholangiocarcinoma [2]. HCC has the characteristics of occult onset, long latency, high malignancy, rapid progression, strong invasion, easy metastasis,

and poor prognosis [3]. Therefore, it is important for the development of tumor immunotherapy to find a key signal pathway to regulate tumor-associated myeloid cells.

The OX2 membrane glycoprotein (CD200) is expressed on a broad range of tissues, including lymphoid cells, neurons, and endothelium [13]. Previous studies have shown that the

interaction of CD200 and CD200R may play an important role in tumor growth and deterioration [14–16]. CD200 is a member of the Ig superfamily, which contains 2 extracellular Ig domains and an unknown intracellular segment motif, and is expressed on the surface of B cells and activated T cells [17–20]. CD200R, the receptor of CD200, was also a member of the Ig superfamily and is mainly expressed in neutrophils, macrophages, and rod cells [21,22]. Previous studies have shown that CD200 is expressed in a variety of cancer cells and shows tumorigenesis effects [23,24]. Activation of CD200R in macrophages can inhibit autologous immune response [25,26]. These results suggest that the CD200/CD200R signaling pathway is involved in suppressing the function of myeloid cells.

The initial CD4⁺T cells mainly differentiate into auxiliary T cells 1 (Th1) and auxiliary T cells 2 (Th2), which can separate intracellular and extracellular pathogens and secrete inflammatory factors, thereby promoting tumor pathogenesis [27,28]. The initial CD4⁺T cells can also be differentiated into regulatory T cells (Treg cells) and helper T cells 17 (Th17). According to the function of cells, 4 different CD4⁺T cell subsets – Th1, Th2, Thl7, and regulatory Treg – have been demonstrated to date [29,30].

To further study the role of the CD200/CD200R pathway in the carcinogenesis of liver cancer, we carried out in-depth research. We found that CD200R inhibitor suppressed the growth of tumors and decreased the levels of Th17 and Treg in peripheral blood. These results are consistent with previous research. Tregs constitutively express the intracellular transcription factor Foxp3 [31]. We found that the expression of Foxp3 was increased in tumor tissues and CD200R inhibitor decreased the level of Foxp3.

## Conclusions

The CD200/CD200R signaling pathway participates in the growth of HCC and regulates the numbers of Th1, Th17, and Treg cells in HCC. The recurrence of HCC was effectively inhibited by thermal ablation treatment. Our results suggest a potential therapy for HCC.

### Conflict of interest

None.

## References:

1. Wong KK, Zhu F, Khatri I et al: Characterization of CD200 ectodomain shedding. PLoS One, 2016; 11: e0152073

2. Clark DA, Dhesy-Thind S, Arredondo JL et al: The receptor for the CD200 tolerance-signaling molecule associated with successful pregnancy is expressed by early stage breast cancer cells in 80% of patients and by term placental trophoblasts. Am J Reprod Immunol, 2015; 74: 387–91

3. Overgaard J: Influence of extracellular pH on the viability and morphology of tumor cells exposed to hyperthermia. J Natl Cancer Inst, 1976; 56(6): 1243–50

4. Richter K, Haslbeck M, Buchner J: The heat shock response: Life on the verge of death. Mol Cell, 2010; 40(2): 253–66

5. Wong MC, Jiang JY, Goggins WB et al: International incidence and mortality trends of liver cancer: A global profile. Sci Rep, 2017; 7: 45846

6. Ali MY, Grimm CF, Ritter M et al: Activation of dendritic cells by local ablation of hepatocellular carcinoma. J Hepatol, 2005; 43(5): 817–22

7. Wang LQ, Yan CF, Zhao Y et al: Reduced CD200 and CD200R1 expression in human chorionic villi contributes to early spontaneous abortion. Acta Obstet Gynecol Scand, 2014; 93: 1248–54

8. Nathan C, Muller WA: Putting the brakes on innate immunity: A regulatory role for CD200? Nat Immunol, 2001; 2: 17–19

9. Rygiel TP, Karnam G, Goverse G: CD200-CD200R signaling suppresses anti-tumor responses independently of CD200 expression on the tumor. Oncogene, 2012; 31: 2979–88

10. Yu G, Sun Y, Foerster K: LPS-induced murine abortions require C5 but not C3, and are prevented by upregulating expression of the CD200 tolerance signaling molecule. Am J Reprod Immunol, 2008; 60: 135–40

11. Clark DA, Ding JW, Yu G et al: Fgl2 prothrombinase expression in mouse trophoblast and deciduas triggers abortion but may be countered by OX-2. Mol Hum Reprod, 2001; 7: 185–94

12. Clark DA, Arredondo JL, Dhesy-Thind S: The CD200 tolerance signaling molecule and its receptor, CD200R1, are expressed in human placental villus trophoblast and in peri-implant decidua by 5 weeks gestation. J Reprod Immunol, 2016; 117: 89–90

13. Xin L, Ertel JM, Rowe JH: Cutting edge: committed Th1 CD4+ T cell differentiation blocks pregnancy-induced Foxp3 expression with antigen-specific fetal loss. J Immunol, 2014; 182: 2970–74

14. Toda Y, Tsakada J, Misago M et al: Autocrine induction of the human pro-IL-1-β gene promoter by IL-1β in monocytes. J Immunol, 2002; 168: 1984–91

15. Hernangomez M, Mestre L, Correa FG et al: CD200-CD200R1 interaction contributes to neuroprotective effects of anandamide on experimentally induced inflammation. Glia, 2012; 60: 1437–50

16. Chen Z, Chen DX, Kai Y et al: Identification of an expressed truncated form of CD200, CD200tr, which is a physiologic antagonist of CD200-induced suppression. Transplantation, 2008; 86: 1116–24

17. Chen Z, Ma X, Zhang J et al: Alternative splicing of CD200 is regulated by an exonic splicing enhancer and SF2/ASF. Nucleic Acids Res, 2010; 38: 6684–96

18. Chitnis T, Imitola J, Wang Y et al: Elevated neuronal expression of CD200 protects Wlds mice from inflammation-mediated neurodegeneration. Am J Pathol, 2007; 170: 1695–712

19. Dentesano G, Serratosa J, Tusell JM et al: CD200R1 and CD200 expression are regulated by PPAR-γ in activated glial cells. Glia, 2014; 62: 982–98

20. Dentesano G, Straccia M, Ejarque-Ortiz A et al: Inhibition of CD200R1 expression by C/EBPβ in reactive microglial cells. J Neuroinflamm, 2012; 9: 165

21. Hatherley D, Barclay AN: The CD200 and CD200 receptor cell surface proteins interact through their N-terminal immunoglobulin-like domains. Eur J Immunol, 2004; 34: 1688–94

22. Hernangómez M, Mestre L, Correa F et al: CD200-CD200R1 interaction contributes to neuroprotective effects of anandamide on experimentally induced inflammation. Glia, 2012; 60: 1437–50

23. Hoek RM, Ruuls SR, Murphy CA et al: Down-regulation of the macrophage lineage through interaction with OX2 (CD200). Science, 2000; 290: 1768–71

24. Koning N, Swaab DF, Hoek RM, Huitinga I: Distribution of the immune inhibitory molecules CD200 and CD200R in the normal central nervous system and multiple sclerosis lesions suggested neuron-glia and glia-glia interactions. J Neuropathol Exp Neurol, 2009; 68: 159–67

25. Liu Y, Bando Y, Vargas-Lowy D et al: CD200R1 agonist attenuates mechanisms of chronic disease in a murine model of multiple sclerosis. J Neurosci, 2010; 30: 2025–38

26. Erin N, Podnos A, Tanriover G et al: Bidirectional effect of CD200 on breast cancer development and metastasis, with ultimate outcome determined by tumor aggressiveness and a cancer-induced inflammatory response. Oncogene, 2015; 34(29): 3860–70

27. Zhang R, Zeng H, Zhang Y et al: CD226 ligation protects against EAE by promoting IL-10 expression via regulation of CD4+ T cell differentiation. Oncotarget, 2016; 7: 19251–64

28. Luchtman DW, Ellwardt E, Larochelle C, Zipp F: IL-17 and related cytokines involved in the pathology and immunotherapy of multiple sclerosis: Crrent and future developments. Cytokine Growth Factor Rev, 2014; 25: 403–13

29. Zhang J, Cheng Y, Cui W et al: MicroRNA-155 modulates Th1 and Th17 cell differentiation and is associated with multiple sclerosis and experimental autoimmune encephalomyelitis. J Neuroimmunol, 2014; 266: 56–63

30. Du C, Liu C, Kang J et al: MicroRNA miR-326 regulates TH-17 differentiation and is associated with the pathogenesis of multiple sclerosis. Nat Immunol, 2009; 10: 1252–59

31. Song HP, Liu SJ, Zhao ZY et al: Increased cycles of DC/CIK immunother-apy decreases frequency of Tregs in patients with resected NSCLC. Int Immunopharmacol, 2017; 52: 197–202